

Article

# In-Situ FT-IR Spectroscopy Investigation of CH<sub>4</sub> and CO<sub>2</sub> Reaction

Yongjun Liu <sup>1</sup>, Nan Cui <sup>1</sup>, Penglong Jia <sup>1</sup> and Wei Huang <sup>1,2,\*</sup>

<sup>1</sup> Key Laboratory of Coal Science and Technology of Ministry of Education and Shanxi Province, Taiyuan University of Technology, Taiyuan 030024, China; liuyongjun@tyut.edu.cn (Y.L.); cuinan1030@163.com (N.C.); jiapenglong0720@163.com (P.J.)

<sup>2</sup> Coal Conversion Engineering Technology Company of TYUT, Taiyuan 030024, China

\* Correspondence: huangwei@tyut.edu.cn; Tel./Fax: +86-351-601-8073

Received: 10 December 2019; Accepted: 12 January 2020; Published: 16 January 2020



**Abstract:** An exclusive trace of CH<sub>4</sub> direct carboxylation with CO<sub>2</sub> by a stepwise technology was investigated using in-situ FT-IR spectroscopy. The results showed that CH<sub>4</sub> was dissociated to atomic hydrogen and M-CH<sub>x</sub> species on catalyst surface when it was first introduced in the system, then CO<sub>2</sub> was inserted into the intermediate to direct carboxylate. Finally, the subsequent adsorption of CH<sub>4</sub> provided active hydrogen for the species of previous surface reaction, thus leading to the formation of the product. It was also found that the first introduction of CO<sub>2</sub> on the surface of the “clean” catalyst might likely react with surface H species, which had an irreversible effect on the catalytic activity of CH<sub>4</sub>.

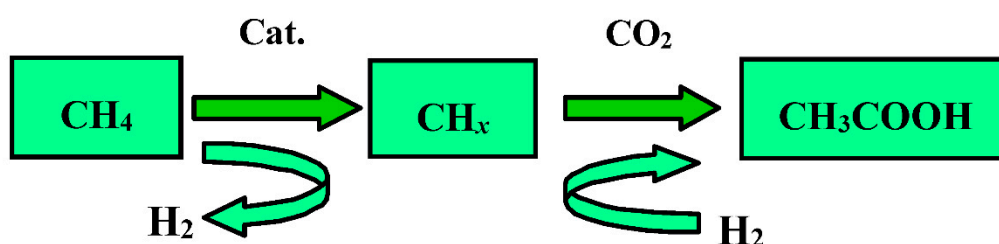
**Keywords:** CH<sub>4</sub>; CO<sub>2</sub>; CH<sub>3</sub>COOH; step-wise route; in-situ FT-IR; Cu-Co

## 1. Introduction

Chemical conversion of CO<sub>2</sub> into value-added fuels and chemicals is regarded as an attractive strategy to simultaneously reduce the CO<sub>2</sub> emissions and relieve the shortage of fossil-fuels both in the energy and chemical industries [1]. To date, much attention has been paid to CO<sub>2</sub> hydrogenation routes [2]. However, the high energy and H<sub>2</sub> consumptions, as well as the rigor operating conditions related to this process, are major challenges.

Instead of using H<sub>2</sub>, the high H/C ratio and abundant reserves of CH<sub>4</sub> make it a viable source of both energy and hydrogen for CO<sub>2</sub> conversion. In fact, CH<sub>4</sub> is an ideal H supplier to replace H<sub>2</sub>, while CO<sub>2</sub> can provide oxygen for the chemical fixation of CH<sub>4</sub>. Thus, the simultaneous conversion of CO<sub>2</sub> and CH<sub>4</sub> to C<sub>2+</sub> oxygenates (e.g., acetic acid) is an ideal combination of a reduction reaction and an oxygenation reaction. Moreover, due to the stoichiometric ratio of C and O atoms, the co-conversion of CO<sub>2</sub> and CH<sub>4</sub> into acetic acid (CO<sub>2</sub> + CH<sub>4</sub> → CH<sub>3</sub>COOH) is 100% atom economy, which can increase the atom utilization and avoid the formation of H<sub>2</sub>O comparing with CO<sub>2</sub> hydrogenation. Unfortunately, the reaction is thermodynamically unfavorable under moderate conditions ( $\Delta G_{298K} = 71.2$  kJ/mol). Many works are devoted to selectively break the C–H bond in CH<sub>4</sub> and simultaneously utilize the inertness of CO<sub>2</sub> to realize C–C coupling for the synthesis of high-value chemicals [3–7]. Most of these works are based on theoretical calculation and experiments which always require additional energy supply (such as plasma), few in-situ characterizations studies have been conducted. Weng et al. [8] employed in-situ time-resolved FT-IR to investigate the partial oxidation of methane to syngas at 500 °C, which indicated that significant different mechanisms were proceeded over supported Rh and Ru catalysts. Besides, the in-situ FT-IR spectroscopy was also conducted to investigate the surface reaction of CH<sub>4</sub> with NO<sub>x</sub> species [9–12].

Our group was committed to investigating the direct conversion of  $\text{CH}_4$  with  $\text{CO}_2$  to acetic acid by stepwise reaction technology (Scheme 1) that bypassed the thermodynamic limitation and demonstrated the feasible and efficient through initial experiments in micro-reactor units at low temperatures over Cu-Co and Co-Pd catalyst [13–15]. However, the possible reaction intermediates in this process had not been elucidated. In addition, to the best of our knowledge, there were no detailed studies focus on direct carboxylation of  $\text{CH}_4$  to investigate the reaction mechanism over Cu-Co catalyst at a lower temperature using in-situ technologies. Therefore, in this study, an exclusive trace of adsorbed  $\text{CH}_4$  direct carboxylation with  $\text{CO}_2$  was performed using the stepwise technology by in-situ FT-IR spectroscopy to gain a deeper understanding of the results of the interaction between  $\text{CH}_4$  and  $\text{CO}_2$ .



**Scheme 1.** Stepwise reaction technology for direct synthesis of  $\text{CH}_3\text{COOH}$  from  $\text{CO}_2$  and  $\text{CH}_4$ .

## 2. Results

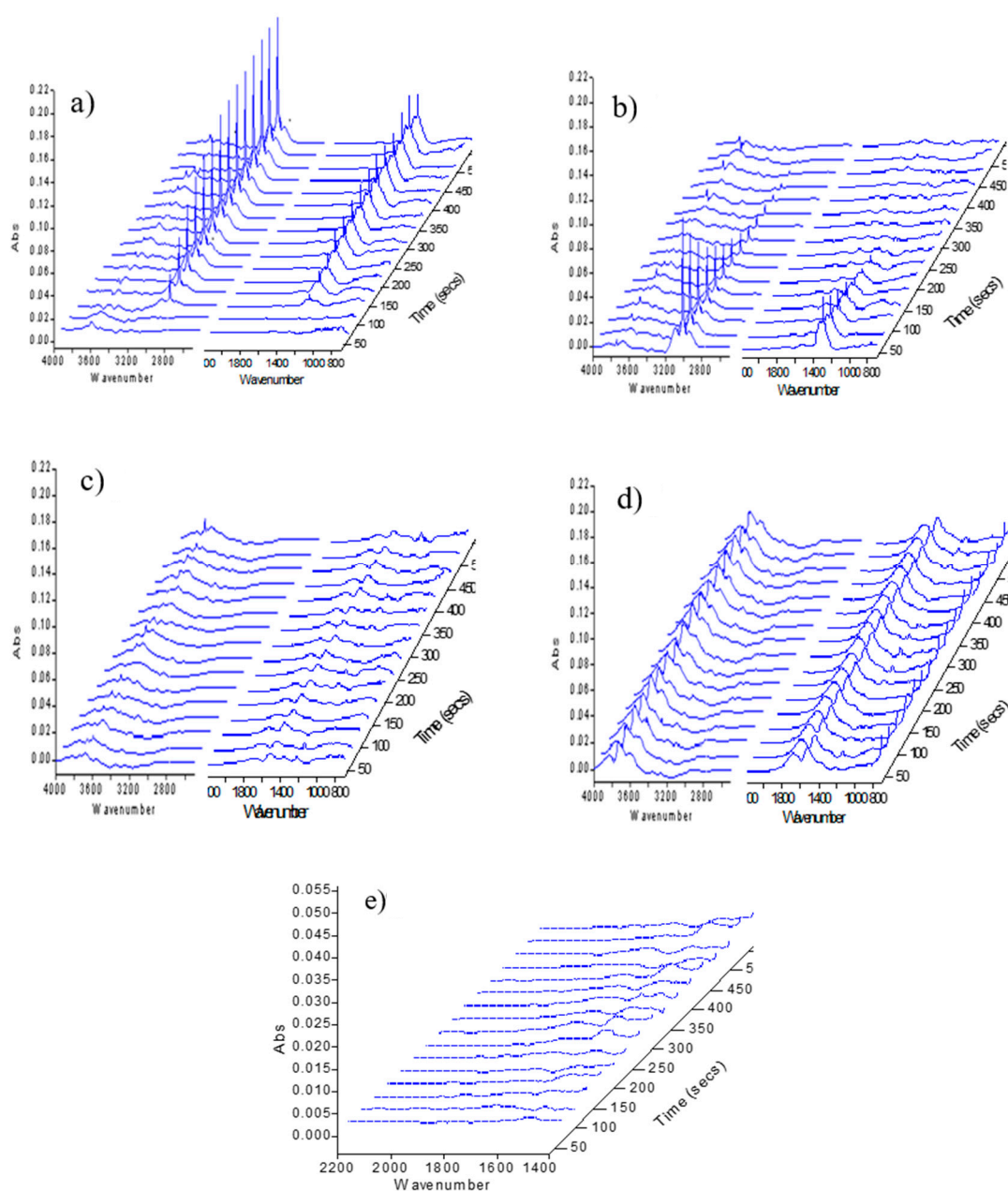
### 2.1. Blank Experiment

Figure 1a showed the FT-IR spectra of pure  $\text{SiO}_2$  (diluent in this experiment) exposed in  $\text{CH}_4$  for the first time after pretreatment in  $\text{N}_2$  for 1 h. The  $\text{SiO}_2$  also underwent the same reduction and purging process under  $\text{N}_2$  atmosphere as that of the catalyst sample. One could see that the intensity of the two main absorption bands at  $3015\text{ cm}^{-1}$  and  $1302\text{ cm}^{-1}$  gradually increased with the introduction of  $\text{CH}_4$ , which was assigned to the adsorption of gas  $\text{CH}_4$  and weak adsorption  $\text{CH}_4$ , respectively [16,17]. Amplification of  $1400\text{ cm}^{-1}$ – $2200\text{ cm}^{-1}$  (see Figure 1e) showed that there were two broad hydroxyl absorption peaks in  $1687\text{ cm}^{-1}$  and  $1524\text{ cm}^{-1}$ , which gradually became clear and stable with the increase of contact time.

Figure 1b was the FT-IR spectra under  $\text{N}_2$  purging after the first cycle of  $\text{CH}_4$  adsorption. It could be seen that the peaks of  $\text{CH}_4$  absorption at  $3015\text{ cm}^{-1}$  and  $1302\text{ cm}^{-1}$  gradually decreased and disappeared, while these OH absorption peaks at  $1687\text{ cm}^{-1}$ ,  $1524\text{ cm}^{-1}$  and  $3200\text{ cm}^{-1}$ – $3800\text{ cm}^{-1}$  slightly increased with the purge of  $\text{N}_2$ . After  $\text{N}_2$  purging, the C–H absorption could hardly be observed at  $2950\text{ cm}^{-1}$  and  $2864\text{ cm}^{-1}$ , indicating that  $\text{CH}_4$  could not be activated on the “clean”  $\text{SiO}_2$ .

After  $\text{N}_2$  purging, the pure  $\text{SiO}_2$  was exposed in  $\text{CO}_2$  for the first time and the corresponding IR spectra was presented in Figure 1c. It could be seen that few changes of the adsorbed species on the surface were observed except at  $1687\text{ cm}^{-1}$  and  $1524\text{ cm}^{-1}$ , indicating that no significant surface reaction had been taken place. In the following series of repetitive cycles, the intensity of peak at  $1690\text{ cm}^{-1}$  and  $1530\text{ cm}^{-1}$  further increased, and two weak peaks at  $2950\text{ cm}^{-1}$  and  $2864\text{ cm}^{-1}$  were found, which might be the result of the interaction between  $\text{CO}_2$  and  $\text{CH}_4$  (Figure 1d).

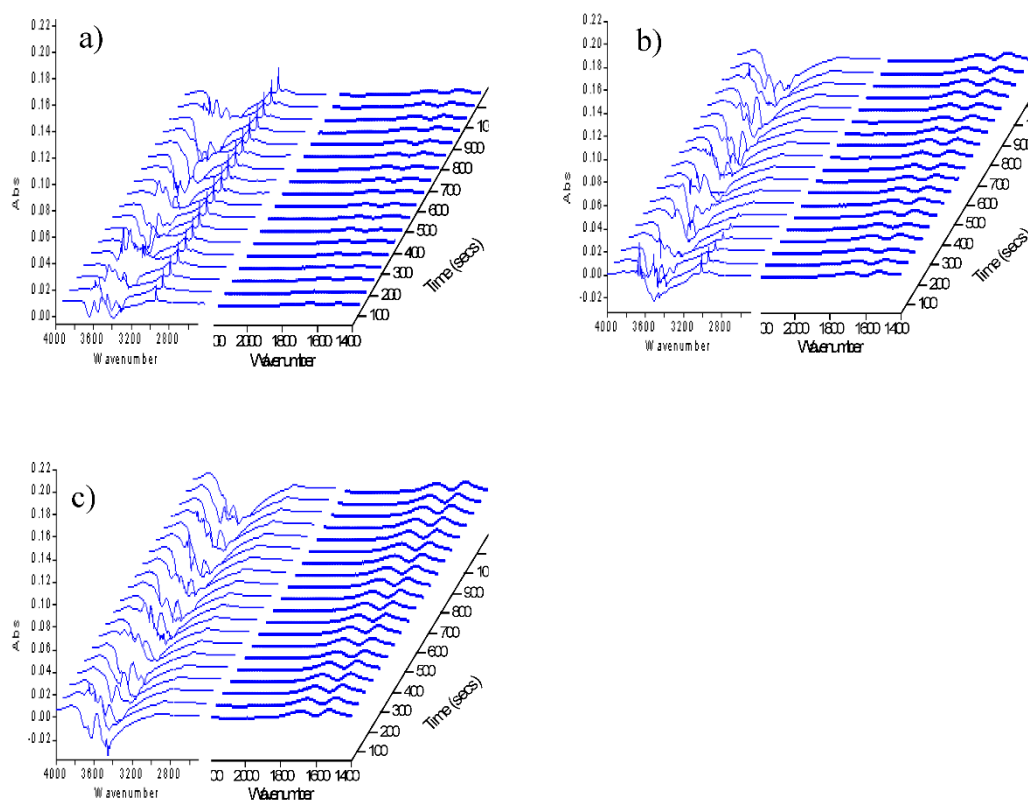
In conclusion, the above experiments demonstrated that the  $\text{CH}_4$  activation and the co-conversion with  $\text{CO}_2$  on pure  $\text{SiO}_2$  were extremely weak under the reaction conditions.



**Figure 1.** FT-IR spectra of SiO<sub>2</sub> exposed in different atmospheres. (a) Exposed in CH<sub>4</sub> for the first time; (b) Exposed in N<sub>2</sub> after the first time of CH<sub>4</sub> adsorption; (c) Exposed in CO<sub>2</sub> for the first time; (d) IR spectra after alternate feeds of CH<sub>4</sub> and CO<sub>2</sub> three times; (e) Amplification of 1400 cm<sup>-1</sup>–2200 cm<sup>-1</sup> when SiO<sub>2</sub> exposed in CH<sub>4</sub> for the first time.

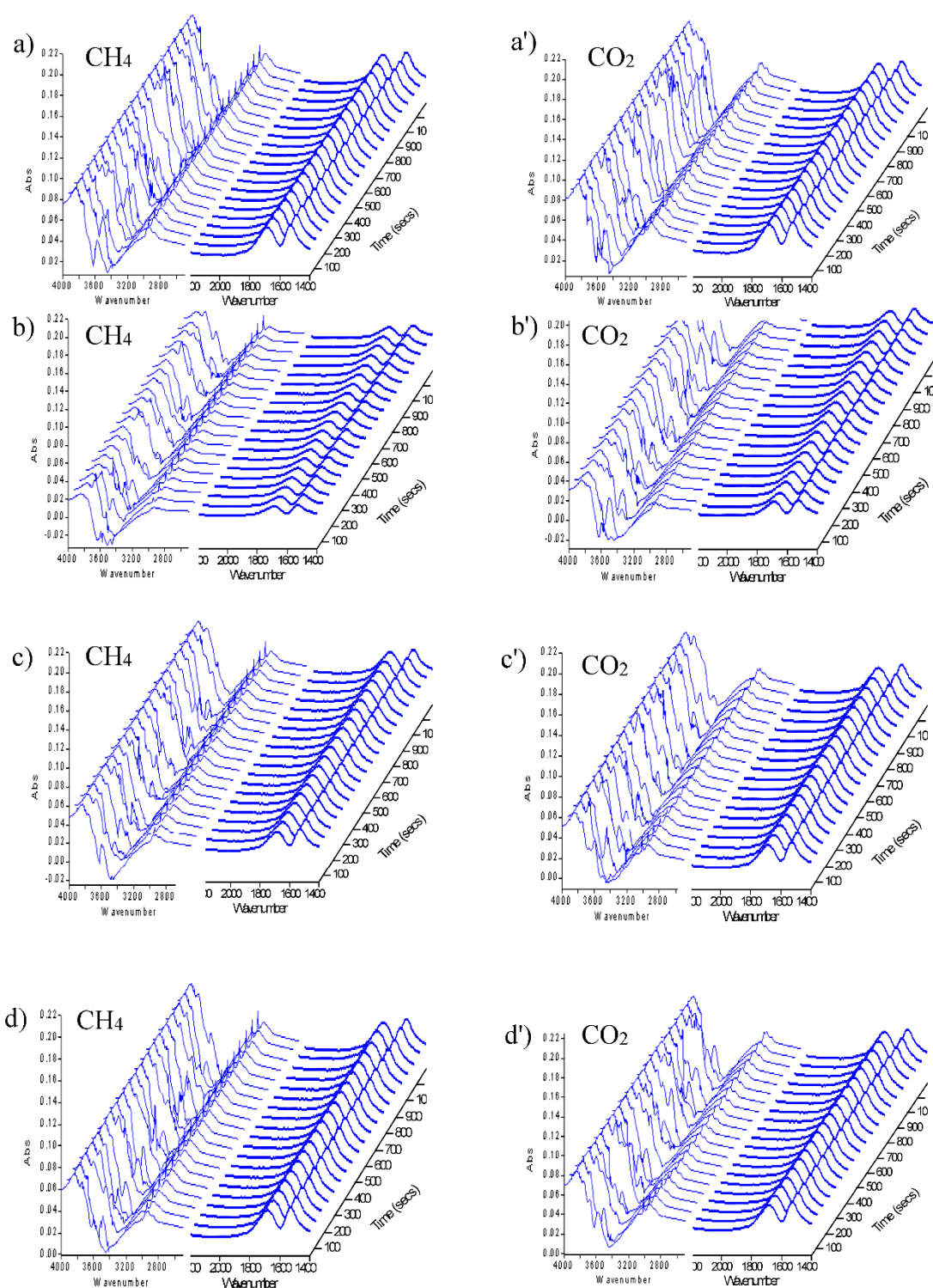
## 2.2. Cu-Co Catalyst Sample Experiment

Figure 2 displayed the FT-IR spectra of Cu-Co catalyst for the first cycle of CH<sub>4</sub> adsorption, N<sub>2</sub> purge, and CO<sub>2</sub> adsorption. As seen, compared with pure SiO<sub>2</sub>, obvious C-H absorption peaks could be observed in the region of 2800 cm<sup>-1</sup>–3000 cm<sup>-1</sup> after the adsorption of CH<sub>4</sub> (see Figure 2a). Besides, the peaks of 1690 cm<sup>-1</sup> and 1530 cm<sup>-1</sup> appeared faster and stronger (Figure 2b). Moreover, with the introduction of CH<sub>4</sub>, negative peaks appeared in the region of 3200 cm<sup>-1</sup>–3800 cm<sup>-1</sup> which belonged to hydroxyl, and the peaks intensity decreased slightly when CO<sub>2</sub> was introduced (Figure 2c). These results suggested that CH<sub>4</sub> had been activated on Cu-Co catalyst surface, which would be discussed later.



**Figure 2.** FT-IR spectra of Cu-Co catalyst exposed in different atmospheres for the first cycle (a) CH<sub>4</sub>; (b) N<sub>2</sub>; (c) CO<sub>2</sub>.

Figure 3 showed the FT-IR spectra of CH<sub>4</sub>/CO<sub>2</sub> repeated feeds. The peaks intensity of 3200 cm<sup>-1</sup>–3800 cm<sup>-1</sup>, 2700 cm<sup>-1</sup>–3000 cm<sup>-1</sup>, and 1400 cm<sup>-1</sup>–1700 cm<sup>-1</sup> continued to increase with CH<sub>4</sub>/CO<sub>2</sub> repeated feeding into the reaction, indicating that the activation and surface reaction of CH<sub>4</sub> and CO<sub>2</sub> were further proceeding. Meanwhile, the results demonstrated that the generated species accumulated on the catalyst surface.



**Figure 3.** FT-IR spectra of CH<sub>4</sub>/CO<sub>2</sub> repeated feed over Cu-Co catalyst. (a,a'): the second cycle; (b,b'): the third cycle; (c,c'): the fourth cycle; (d,d'): the fifth cycle.

### 3. Discussion

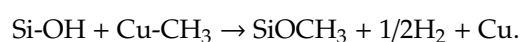
#### 3.1. Activation of CH<sub>4</sub> on "Clean" Catalyst Surface

Generally, the characteristic absorption of C–H bond occurred in three regions: 3000 cm<sup>-1</sup>–2700 cm<sup>-1</sup>, 1475 cm<sup>-1</sup>–1300 cm<sup>-1</sup> and 1000 cm<sup>-1</sup>–650 cm<sup>-1</sup> [18]. Among them, 1000 cm<sup>-1</sup>–650 cm<sup>-1</sup> fell in the fingerprint area, and there were many influence factors that were

complex and difficult to give an unequivocal identification. For  $1475\text{ cm}^{-1}$ – $1300\text{ cm}^{-1}$ , since the  $\text{SiO}_2$  had a strong absorption and coverage, the variation was difficult to observe. Therefore, this study mainly focused on the C–H bond absorption in the region of  $3000\text{ cm}^{-1}$ – $2700\text{ cm}^{-1}$ .

In the first cycle,  $\text{CH}_4$  was introduced after the catalyst was reduced and swept by  $\text{N}_2$  for 1 h. Thus, it was considered that the interaction between  $\text{CH}_4$  and the catalyst was carried out on a “clean” surface, reflecting the activation of  $\text{CH}_4$  by the catalyst itself. Compared with pure  $\text{SiO}_2$ , Figure 2b clearly showed that the bonds in the region of  $2800\text{ cm}^{-1}$ – $3000\text{ cm}^{-1}$  increased significantly on the Cu-Co catalyst, indicating that  $\text{CH}_4$  had been activated by the catalyst.

With the introduction of  $\text{CH}_4$ , a large negative peak appeared in the OH absorption region at  $3200\text{ cm}^{-1}$ – $3800\text{ cm}^{-1}$  (Figure 2a,b). The intensity of the peak increased with the increase of contact time, while it decreased slightly after the introduction of  $\text{CO}_2$ . The appearance of negative peaks indicated that OH groups were continuously consumed during the process of  $\text{CH}_4$  adsorption and activation. According to the literature [16], it was pointed out that the adsorbed methyl groups on metal sites could react with OH groups and then spilled onto the carrier. In this process, the following reactions were most likely to occur. Take Cu/ $\text{SiO}_2$  as an example:



Therefore, it was suggested that the decrease of surface OH in this study was due to the interaction between surface C-H species and adjacent OH groups, which caused the transition of  $\text{CH}_4$  activation site to inactive site. Obviously, the spillover of these  $\text{CH}_x$  species on the surface favored to empty the metal active sites and thus activated more amount of  $\text{CH}_4$ .

### 3.2. Reaction of Adsorbed $\text{CH}_4$ and $\text{CO}_2$

After the first introduction of  $\text{CH}_4$ , pure  $\text{N}_2$  was purged to remove the free and weakly adsorbed  $\text{CH}_4$  for 20 min,  $\text{CO}_2$  was then introduced to investigate the reaction between  $\text{CO}_2$  and surface species. Rasko and Solymosi [19,20] studied the reaction of  $\text{CH}_3$  species (formed by the decomposition of diazomethane) with  $\text{CO}_2$  on different carriers and metal surfaces. The results showed that the adsorbed  $\text{CH}_3$  species could react with  $\text{CO}_2$  to produce CO and  $\text{H}_2\text{O}$  under very mild conditions even at room temperature. The reason was that the introduction of  $\text{CO}_2$  led to the decrease or even disappearance of the  $\text{CH}_3$  species peak at  $2800\text{ cm}^{-1}$ – $3000\text{ cm}^{-1}$ , and the generation of CO also could be detected. However, in our study, the introduction of  $\text{CO}_2$  did not lead to the consumption of adsorbed  $\text{CH}_x$  species. On the contrary, these  $\text{CH}_x$  species increased. The results indicated that, on the one hand, there was no reaction occurred between surface  $\text{CH}_x$  species and  $\text{CO}_2$  to form CO and  $\text{H}_2$  under the used catalyst and experimental conditions. On the other hand, it also suggested that  $\text{CO}_2$  might react with surface H species deriving from  $\text{CH}_4$  activation, which led to the rise of surface hydroxyl species. The two aspects were consistent with our previous experimental results [13].

### 3.3. Activation of $\text{CH}_4$ on “Polluted” Catalyst Surface

The adsorption and activation of  $\text{CH}_4$  on the “polluted” catalyst surface could be divided into two situations: One was that the surface of the reduced “clean” catalyst was first filled with  $\text{CO}_2$ , and then  $\text{CH}_4$  was introduced after  $\text{N}_2$  purge for 20 min. Another was that  $\text{CH}_4$  was re-introduced after a cycle of reaction, at which time the catalyst surface was adsorbed by  $\text{CO}_2$ . Figure 4a was the FT-IR spectra when  $\text{CO}_2$  was first introduced. It was shown that no  $\text{CH}_x$  species were formed on the surface of “clean” catalysts when  $\text{CO}_2$  was first introduced, suggesting that there was no adsorbed hydrogen on the catalyst surface after reduction and  $\text{N}_2$  purging process for 1 h, thus no hydrogenation reaction occurred. When  $\text{CH}_4$  was introduced, surface  $\text{CH}_x$  species were generated (Figure 4b). Compared with the first introduction of  $\text{CH}_4$ , the intensity and peak type of  $\text{CH}_x$  species changed greatly, while the peak position had negligible changes. Although no strict quantitative determination had been made in this experiment, the ratio of catalyst and diluent in each sample was almost the same. Thus, it

was concluded that the decrease in the peak area of  $\text{CH}_x$  species was caused by the first adsorption of  $\text{CO}_2$ . Considering that the position of CH adsorption peak moved from  $2939\text{ cm}^{-1}$  to  $2963\text{ cm}^{-1}$ , it was considered that the first introduction of  $\text{CO}_2$  led to the oxidation of catalyst active components.

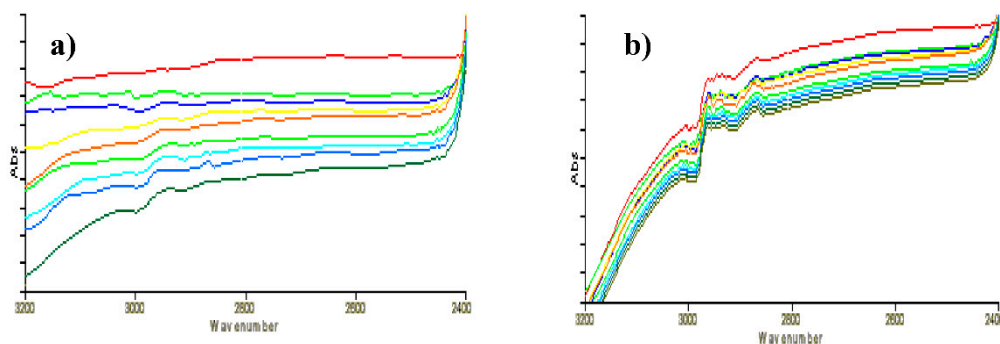


**Figure 4.** FT-IR spectra of “clean” catalyst surface (a) first exposed in  $\text{CO}_2$ ; (b) first exposed in  $\text{CO}_2$  and then in  $\text{CH}_4$ .

The peak intensity of  $\text{CH}_x$  species with the introduction of  $\text{CH}_4$  in different cycles was presented in Figure 5. It could be seen that the peak intensity of  $\text{CH}_x$  species increased linearly in the first cycle, whereas the peak intensity first decreased and then increased for other cycles. This was mainly due to that the first cycles occurred on the “clean” surface of the catalyst, while the adsorption and activation of  $\text{CH}_4$  were carried out on a “non-clean” surface for others. Obviously, on the “polluted” catalyst surface, the subsequent passing of  $\text{CH}_4$  provided hydrogen for the hydrogen-deficient species generated in the previous cycle. Meanwhile, one also could see that the degree of reduction increased with the accumulation of  $\text{CH}_x$  species on the surface, which indicated that the desorption of these  $\text{CH}_x$  species occurred on the catalyst surface. These results explained the formation of  $\text{CH}_3\text{COOH}$ ,  $\text{HCOOH}$  and other oxygenated products without the condition of  $\text{H}_2$  supplementation using the stepwise technology. Obviously, it could be inferred that the direct conversion of  $\text{CH}_4$  and  $\text{CO}_2$  to  $\text{CH}_3\text{COOH}$  by two-step reaction without hydrogen replenishment was due to that the subsequent adsorption of  $\text{CH}_4$  provided thermodynamic power for the previous step, thus leading to the formation of products, which was also consistent with our previous experimental results [13]. The relevant reaction process could be described as follows:



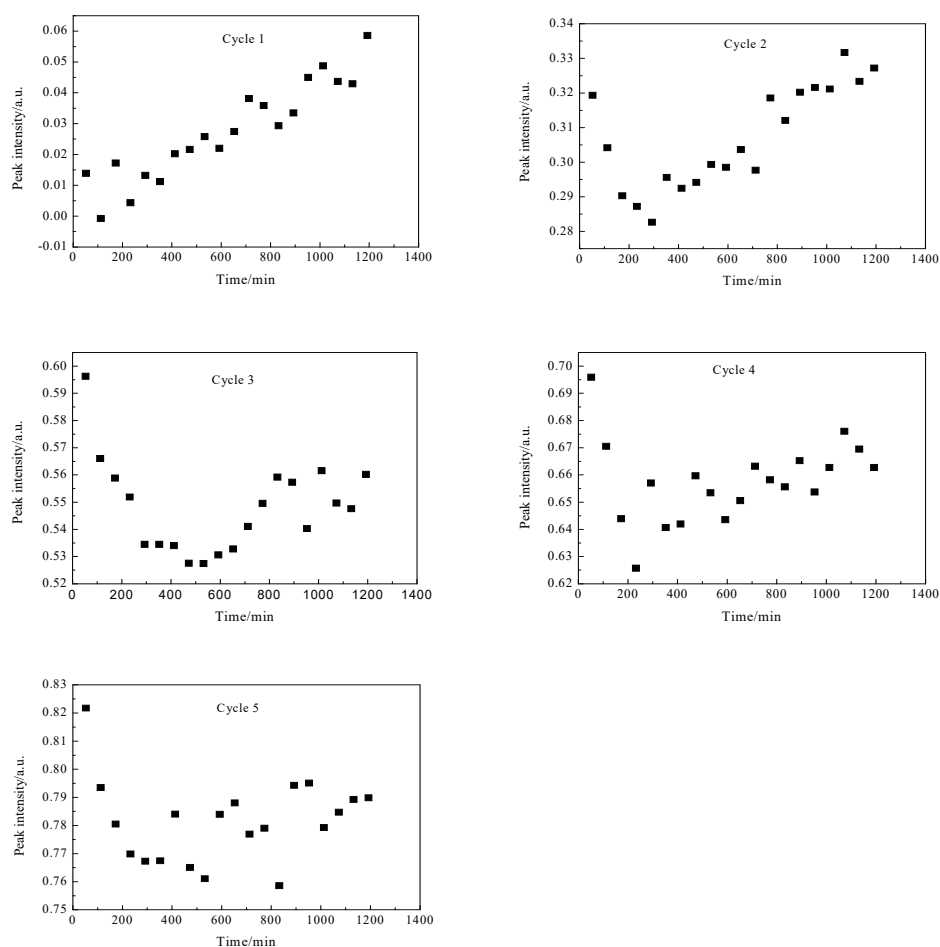


Figure 5. The peak intensity of CH<sub>x</sub> species as a function of CH<sub>4</sub> introduction in different cycles.

## 4. Experimental

### 4.1. Catalyst Preparation

Cu-Co catalyst was synthesized by a co-precipitation method. The Cu:Co atomic ratio in the starting solution was kept at 1:1. Typically, two aqueous solutions, a solution of Cu(II), Co(II) nitrates (analytical reagent, Tianjin, China) and a mixed solution of Na<sub>2</sub>CO<sub>3</sub> (analytical reagent, Tianjin, China) precipitant, were added dropwise to 250 mL of deionized water under vigorous stirring. The pH value was maintained at 6–8. The precipitate was aged at 343 K for 1 h under stirring, and filtered, washed, dried at 393 K for 16 h, and then calcined at 623 K for 6 h. The as-synthesized catalyst was crushed and sieved to particles in the range of 40–60 meshes before use.

### 4.2. Test of In-Situ FT-IR

The in-situ FT-IR experiments were performed on a Perkin Elmer Spectrum 2000 FT-IR spectrometer (PerkinElmer, USA). The above catalyst was mixed with high purity SiO<sub>2</sub> to make thin sheets and placed in in-situ IR cells for the test. Before the experiment, the catalyst was reduced in 10% H<sub>2</sub>/N<sub>2</sub> at a flow rate of 20 mL/min under atmospheric pressure. The reduction temperature was programmed to increase from room temperature to 473 K with a heating rate of 5 K/min and maintained at 473 K for 2 h. After reduction, the reaction system was purged with N<sub>2</sub> at 473 K for 1 h. Then CH<sub>4</sub> and CO<sub>2</sub> were alternately switched to react, during which N<sub>2</sub> was purged with 20 min or not. At the same time, the spectral data were recorded using TimeBase software (PerkinElmer company, MA, USA) at the frequency of one graph per minute.



## 5. Conclusions

In conclusion, a possible reaction mechanism for the direct conversion of CH<sub>4</sub> and CO<sub>2</sub> to CH<sub>3</sub>COOH by a step-wise technology had been proposed based on the in-situ FT-IR spectroscopy. Results showed that CH<sub>4</sub> was dissociated to atomic hydrogen and M-CH<sub>x</sub> species on catalyst surface when it was first introduced in the system, then CO<sub>2</sub> was inserted into the intermediate to direct carboxylate. Finally, the subsequent CH<sub>4</sub> adsorption provided active hydrogen for the species of previous surface reaction, thus leading to the formation of the product. The activated CH<sub>4</sub> also could be transferred to unreduced oxides through interaction with adjacent hydroxyl groups, which favored to empty the metal active sites and thus greatly enhanced the catalytic activity of CH<sub>4</sub>. However, the first introduction of CO<sub>2</sub> on the surface of the “clean” catalyst might likely react with surface H species, which had an irreversible effect on the catalytic activity of CH<sub>4</sub>.

**Author Contributions:** The experimental work was designed and supported by W.H. Y.L., analyzed the data and write the original article. N.C. and P.J. prepared the catalyst and conduct the experiment. All authors have read and agreed to the published version of the manuscript.

**Funding:** This research was supported by the Key Project of National Natural Science Foundation of China (21336006), the National Natural Science Foundation of China (21908157), the Natural Science Younger Foundation of Shanxi Province (201801D221076) and the Key R&D Program of Shanxi Province (201803D121043).

**Conflicts of Interest:** The authors declare no conflict of interest.

## References

1. Song, Q.W.; Zhou, Z.H.; He, L.N. Efficient, selective and sustainable catalysis of carbon dioxide. *Green Chem.* **2017**, *19*, 3707–3728. [[CrossRef](#)]
2. Álvarez, A.; Bansode, A.; Urakawa, A.; Bavykina, A.V.; Wezendonk, T.A.; Makkee, M.; Gascon, J.; Kapteijn, F. Challenges in the greener production of formates/formic acid, methanol, and DME by heterogeneously catalyzed CO<sub>2</sub> hydrogenation processes. *Chem. Rev.* **2017**, *117*, 9804–9838. [[CrossRef](#)] [[PubMed](#)]
3. Zhao, Y.T.; Wang, H.; Han, J.Y.; Zhu, X.L.; Ge, Q.F. Active site ensembles enabled C-C coupling of CO<sub>2</sub> and CH<sub>4</sub> for acetone production. *J. Phys. Chem. C* **2018**, *122*, 9570–9577. [[CrossRef](#)]
4. Zhao, Y.T.; Cui, C.N.; Han, J.Y.; Wang, H.; Zhu, X.L.; Ge, Q.F. Direct C-C coupling of CO<sub>2</sub> and the methyl group from CH<sub>4</sub> activation through facile insertion of CO<sub>2</sub> into Zn-CH<sub>3</sub> σ-Bond. *J. Am. Chem. Soc.* **2016**, *138*, 10191–10198. [[CrossRef](#)] [[PubMed](#)]
5. Wang, L.; Yi, Y.H.; Wu, C.F.; Guo, H.C.; Tu, X. One-step reforming of CO<sub>2</sub> and CH<sub>4</sub> into high-value liquid chemicals and fuels at room temperature by plasma-driven catalysis. *Angew. Chem. Int. Ed.* **2017**, *56*, 13679–13683. [[CrossRef](#)] [[PubMed](#)]
6. Montejo-Valencia, B.D.; Pagan-Torres, Y.J.; Martínez-Inesta, M.M.; Curet-Arana, M.C. Density functional theory (DFT) study to unravel the catalytic properties of M-exchanged MFI, (M = Be, Co, Cu, Mg, Mn, Zn) for the conversion of methane and carbon dioxide to acetic acid. *ACS Catal.* **2017**, *7*, 6719–6728. [[CrossRef](#)]
7. Shavi, R.; Ko, J.; Cho, A.; Han, J.W.; Seo, J.G. Mechanistic insight into the quantitative synthesis of acetic acid by direct conversion of CH<sub>4</sub> and CO<sub>2</sub>: An experimental and theoretical approach. *Appl. Catal. B Environ.* **2018**, *229*, 237–248. [[CrossRef](#)]
8. Weng, W.Z.; Chen, M.S.; Yan, Q.G.; Wu, T.H.; Chao, Z.S.; Liao, Y.Y.; Wan, H.L. Mechanistic study of partial oxidation of methane to synthesis gas over supported rhodium and ruthenium catalysts using in situ time-resolved FTIR spectroscopy. *Catal. Today* **2000**, *63*, 317–326. [[CrossRef](#)]
9. Lobree, L.J.; Aylor, A.W.; Reimer, J.A.; Bell, A.T. NO reduction by CH<sub>4</sub> in the presence of O<sub>2</sub> over Pd-H-ZSM-5. *J. Catal.* **1999**, *181*, 189–204. [[CrossRef](#)]
10. Kantcheva, M.; Cayirtepe, I. FT-IR spectroscopic investigation of the surface reaction of CH<sub>4</sub> with NO<sub>x</sub> species adsorbed on Pd/WO<sub>3</sub>-ZrO<sub>2</sub> catalyst. *Catal. Lett.* **2007**, *115*, 148–162. [[CrossRef](#)]
11. Kantcheva, M.; Vakkasoglu, A.S. Cobalt supported on zirconia and sulfated zirconia I.: FT-IR spectroscopic characterization of the NO<sub>x</sub> species formed upon NO adsorption and NO/O<sub>2</sub> coadsorption. *J. Catal.* **2004**, *223*, 352–363. [[CrossRef](#)]

12. Tsyntsarski, B.; Averska, V.; Kolev, H.; Marinova, T.; Klissurski, D.; Hadjiivanov, K. FT-IR study of the nature and reactivity of surface NO<sub>x</sub> compounds formed after NO adsorption and NO + O<sub>2</sub> coadsorption on zirconia- and sulfated zirconia-supported cobalt. *J. Mol. Catal. A* **2003**, *193*, 139–149. [[CrossRef](#)]
13. Huang, W.; Xie, K.C.; Wang, J.P.; Gao, Z.H.; Yin, L.H.; Zhu, Q.M. Possibility of direct conversion of CH<sub>4</sub> and CO<sub>2</sub> to high-value products. *J. Catal.* **2001**, *201*, 100–104. [[CrossRef](#)]
14. Huang, W.; Sun, W.Z.; Li, F. Efficient synthesis of ethanol and acetic acid from methane and carbon dioxide with a continuous, stepwise reactor. *AIChE J.* **2010**, *56*, 1279–1284. [[CrossRef](#)]
15. Ding, Y.H.; Huang, W.; Wang, Y.G. Direct synthesis of acetic acid from CH<sub>4</sub> and CO<sub>2</sub> by a step-wise route over Pd/SiO<sub>2</sub> and Rh/SiO<sub>2</sub> catalysts. *Fuel Process. Technol.* **2007**, *88*, 319–324. [[CrossRef](#)]
16. Driessen, M.D.; Grassian, V.H. Methyl spillover on silica-supported copper catalysts from the dissociative adsorption of methyl halides. *J. Catal.* **1996**, *161*, 810–818. [[CrossRef](#)]
17. Wu, T.H.; Lin, D.M.; Wu, Y.; Zhou, X.P.; Yan, Q.G.; Weng, W.Z.; Wan, H.L. In-situ FT-IR investigation of partial oxidation of methane to syngas over Rh/SiO<sub>2</sub> catalyst. *J. Nat. Gas Chem.* **2007**, *16*, 316–321. [[CrossRef](#)]
18. Srivastava, A.K.; Pandey, A.K.; Jain, S.N. FT-IR spectroscopy, intra-molecular CHO interactions, HOMO, LUMO, MESP analysis and biological activity of two natural products, triclisine and rufescine: DFT and QTAIM approaches. *Misra Spectrochim. Acta A* **2015**, *136*, 682–689. [[CrossRef](#)] [[PubMed](#)]
19. Raskó, J.; Solymosi, F. Reactions of adsorbed CH<sub>3</sub> species with CO<sub>2</sub> on Rh/SiO<sub>2</sub> catalyst. *Catal. Lett.* **1997**, *46*, 153–157. [[CrossRef](#)]
20. Raskó, J.; Solymosi, F. Adsorption of CH<sub>3</sub> and its reactions with CO<sub>2</sub> over TiO<sub>2</sub>. *Catal. Lett.* **1998**, *54*, 49–54. [[CrossRef](#)]



© 2020 by the authors. Licensee MDPI, Basel, Switzerland. This article is an open access article distributed under the terms and conditions of the Creative Commons Attribution (CC BY) license (<http://creativecommons.org/licenses/by/4.0/>).